# Pseudo-linear Variable Lever Variable Stiffness Actuator: Design and Evaluation

Miha Dežman and Andrej Gams

Abstract—This paper presents the design, mathematical model, and evaluation of a novel variant of a variable stiffness actuator. The actuator combines a cam and a variable lever mechanism. The lever length changes through the rotation of the follower and results in the change of the mechanism stiffness. The design of the actuator results in a nearly linear torque-deflection characteristic, earning it its name: pseudo-linear variable lever variable stiffness actuator (PLVL-VSA).

The paper outlines the differences to other similar types of variable stiffness mechanisms, namely the pseudo-linear torque-deflection characteristics, no pretensioning of the elastic element and a fast rate of stiffness variation. Provided are the details on the mechanical design and the derivation of the mathematical model. The theoretically calculated pseudo-linear torque-deflection characteristic is shown on a real-world PLVL-VSA built using rapid prototyping, which also displays the rapid rate of stiffness change.

### I. INTRODUCTION

The amount of research in the field of variable stiffness actuators is steadily increasing, leading to predictions that the next generation of robots will use variable compliance hardware [1]. Such hardware can introduce several benefits for both the robots and the users, i.e., easier interaction, increased safety and better energy efficiency [2]. Despite the increased complexity of these mechanisms, when compared to stiff robots, this topic still offers many opportunities for improvement and simplification [3].

Literature describes different kinds of mechanisms all with their advantages and disadvantages. We refer the reader to several review papers on the topics for details [4]–[6]. These focus on describing different architecture types and principles of various mechanisms, thus providing a wider research scope. The work [6] also describes potential applications that can benefit from variable compliance actuators. Examples include safe industrial robots able to work in close proximity to humans, naturally moving toys that are less prone to damage, rehabilitation robots using compliance to achieve different levels of assistance and as a result improve the patient's recovery, robotic prosthesis, walking and running robots, etc. All the listed applications depend on the properties of the used variable stiffness actuators.

In this paper we propose a novel variant of stiffness variation mechanism for a variable stiffness actuator. We also explore several favorable design properties, including no pretension of the elastic element, which reduces the force needed to vary the mechanism stiffness, and pseudo-linear

Both authors are with the Humanoid and Cognitive Robotics Lab, Dept. of Automation, Biocybernetics and Robotics, Jožef Stefan Institute, Ljubljana, Slovenia. miha.dezman@ijs.si

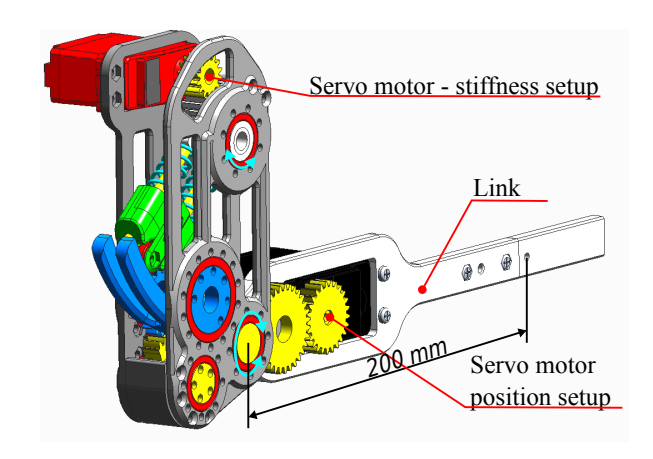


Fig. 1. Virtual model of the PLVL-VSA prototype.

torque-deflection characteristics, which makes control design easier. Torque-deflection characteristics in recognized designs, such as MACCEPA [7] and FSJ-Joint [8], are typically progressive (nonlinear), meaning that with increased deflection the mechanism stiffness rises. However, the nonlinear characteristics can lead to a complex control process [9]. As a drawback, the proposed design suffers from a zero deflection crossing discontinuity. Furthermore, force required to change stiffness at higher deflection angles increases. While the latter is common for VSAs, the former can be significantly reduced with tuning.

This paper is organized as follows. In Section II, a brief comparison is made between a few variable stiffness actuators that relate to our work. Section III focuses on the novel variable stiffness design, its advantages and disadvantages, and the derivation of its mathematical model, based on linear regression. Next, a real-world test prototype of the actuator is described and its characteristics are evaluated in Section IV. Section V provides information about further work and a conclusion.

# II. RELATED WORK

An exact comparison between different variable stiffness actuators is difficult due to a huge amount of available principles, components, parameters and applications. Several guidelines have been proposed in [1]. In this paper, we try to provide a general comparison and point out the design differences between our concept and other mechanisms found in the literature. Our mechanism combines a variable lever arm and a cam mechanism. A 3-D rendering of its first prototype implementation is shown in Fig. 1. According to [6], our proposed mechanism falls within the group of

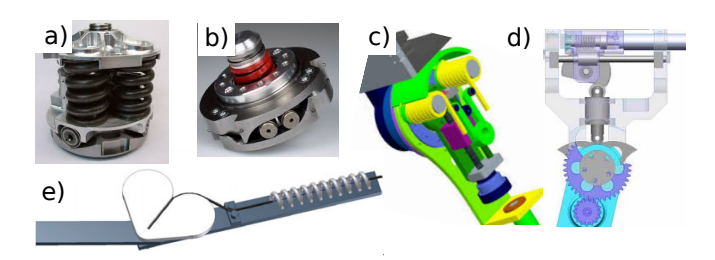


Fig. 2. Various variable stiffness actuators from the literature: a) DLR VS-Joint [10], b) FSJ-Joint [8], c) AwAS-II [12], d) MESTRAN [13] and e) MACCEPA 2.0 [14].

actuators with a mechanically controlled stiffness. Several other mechanisms of such design are for a visual reference shown in Fig. 2.

One example is the VS-Joint [10] and its improved version the FSJ-Joint [8]. Both use a variable spring pretension principle [3] to change the mechanism stiffness, and a cam mechanism to deflect the spring. One of the more important properties of cam mechanisms is the pressure angle  $\alpha$  (see Fig. 3). It is defined as the angle between the follower direction of motion (up-down, green arrow in Fig. 3) and the normal at the point of contact between the follower and the cam surface (see Fig. 3). The value of the pressure angle is important as it dictates the forces acting on the follower. Having an angle higher than 30° [11], the side thrust acting on the follower gets big enough to completely prevent it from moving.

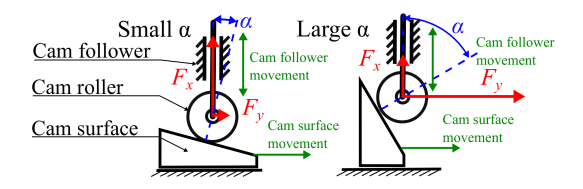


Fig. 3. The difference between a small pressure angle (left) and a large pressure angle (right).

On the other hand, a smaller angle requires a larger force at the follower in order to rotate the cam, which calls for a very stiff pressure spring (e.g., 908 N/mm for VS-Joint [10]). This also affects the achievable deflection angle, torque and maximum storable energy. Relatively high spring forces and spring pretension require a very rigid structure, which is, in turn, heavier and more difficult to manufacture. An advantage of VS-Joint and FSJ-Joint is their very compact cylindrical form, which was chosen for the desired application [15]. However, a more flat form design based on a cam mechanism is also possible. An example of that is the MESTRAN [13].

A different variable spring preload based mechanism is called MACCEPA [7]. In such pretension cases, the stiffness varying motor works in parallel with the stiffness preset mechanism and has to overcome the preload spring force. Consequently, the MACCEPA mechanism offers slower speeds of stiffness change, e. g., 2.6s from 3% to 97% stiffness was reported in [16]. However, this could be accelerated with a more powerful motor. Another issue of the MACCEPA is its highly nonlinear torque-deflection characteristics, which

was taken into consideration with MACCEPA 2.0. There it was improved and adapted to some extent [14]. However, due to a large deflection angle, the MACCEPA is able to store more potential energy than other actuators [17].

Another group of mechanical variable stiffness actuators uses the variable lever principle to achieve variable stiffness. One example is the AwAS-I [18]. It uses a rotational lever placed between two linear pressure springs. Although this mechanism principle is simple and effective, the springs are placed perpendicularly to the lever only at zero deflection. At higher angles, the linear springs get compressed in a nonlinear way making the mathematical model more complex. The use of linear guides is also problematic since they need to withstand the whole force of the spring without mechanical deformations. This increases the required size and weight of this design. However, some of these problems were improved in the second version AwAS-II [12] through torsion springs.

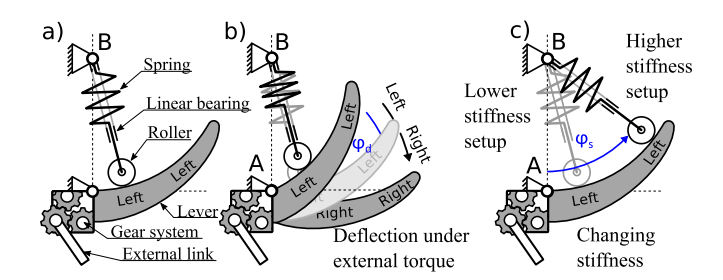
Except for AwAS-I and AwAS-II, the above-listed mechanisms have a highly nonlinear torque-deflection response, which either results from the mechanism principle itself, or mechanism nonlinearities, or both at the same time. A progressive torque-deflection response is often deemed desirable because a stiffening effect helps the actuator avoid reaching the mechanical end-stops when a low stiffness is set [3]. While progressive stiffening will arguably prevent reaching the mechanical end-stop sooner than a linearly stiffening mechanism, it is more challenging to mathematically model and thus makes control more difficult to implement.

Our proposed mechanism design results in a nearly linear torque-deflection characteristic. It most closely resembles the AWAS-I [18] and AWAS-II [12]. The main difference is that the stiffness change in our case is implemented rotationally, whereas the stiffness change in AWAS-I or AWAS-II is implemented linearly. Since in our case stiffness variation is perpendicular to the force of the spring, the speed of stiffness variation can be faster as in mechanisms using spring preload, e.g., the MACCEPA. A rotational stiffness change is easier to implement mechanically, compared to a linear one, as is in, e.g., AWAS-I and AWAS-II. Additionally, only one linear pressure spring is needed in order to operate.

# III. PSEUDO-LINEAR VARIABLE LEVER VARIABLE STIFFNESS ACTUATOR (PLVL-VSA)

#### A. Working principle

The working principle of our mechanism is a combination of a cam deflection and a variable lever mechanism, as shown in Fig. 4a. The system is in principle unidirectional. A curved lever arm compresses the spring while it rotates around the pivot A, thus providing a reaction torque to the external load. However, when turning in the opposite direction, the lever arm loses the contact with the cam roller. To make the system bidirectional, a second lever arm was added through a gear system. The gears are located in the pivot A and reverse the movement of both levers and are also connected to an external link (see Fig. 4a). Which lever is loaded depends on the direction of the external force/torque that deflects the external link (see Fig. 4b). To achieve a higher stiffness, the



The working principle of PLVL-VSA: a) equilibrium position, b) deflection under external torque, and c) varying stiffness.

stiffness mechanism can be rotated (see Fig. 4c). This way, the lever length of the mechanism can be changed, which in turn changes the required torque to compress the spring, hence making the mechanism a variable stiffness actuator. Since the lever arm is curved, the spring system can be rotated theoretically without resistance at zero deflection. In reality, one always needs to overcome the friction in bearings. In addition, a tangential force directed toward lower stiffness angles appears at higher deflection angles.

# B. Mathematical model

The system geometry is very straightforward, which means that a mathematical expression connecting the deflection torque  $M_{\rm d}$  and the deflection angle  $\varphi_{\rm d}$  can be derived. To determine it one needs to calculate the spring compression  $d_{ ext{spr}}$  and the pressure angle lpha of the roller mechanism. The deflection torque is the torque that deflects the mechanism for  $\varphi_{\rm d}$  and is opposite and equal to the torque resulting from the interaction of the mechanism's elastic element (the spring),  $M_{\rm d} = -M_{\rm spr}$ . The mechanism principle with variables is shown in Fig. 5.

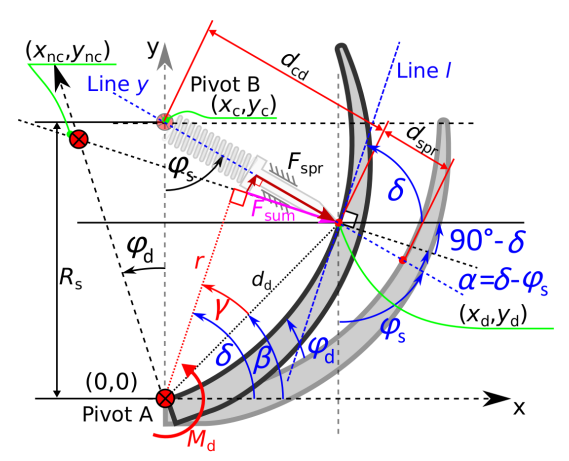


Fig. 5. A flat view of the mechanism principle with relevant variables. The lever is shown in a nominal (transparent) and a deflected position.

The cam profile is that of a circle, which gets rotated around the (0,0) point (pivot A) for the value of the deflection angle  $\varphi_d$ . The spring is at zero deflection angle essentially unloaded at any stiffness angle  $\varphi_s$ . A rigid system is assumed, so no deformations are present except for the spring. In order to determine the spring force  $F_{\rm spr}$ , one first needs to calculate the distance between points  $(x_c, y_c)$  and  $(x_d, y_d)$ , located at the start and the end of the spring, respectively.  $R_{\rm s}$  represents the radius of the cam circle curve, while  $\varphi_{\rm d}$ is the passive deflection (deflection angle). From Fig. 5 we find  $(x_c = 0, y_c = R_s)$ . Under deflection, the center of the cam circle curve moves to coordinates

$$x_{\rm nc} = \cos(\varphi_{\rm d}) \cdot x_{\rm c} - \sin(\varphi_{\rm d}) \cdot y_{\rm c}, \tag{1}$$

$$y_{\rm nc} = \sin(\varphi_{\rm d}) \cdot x_{\rm c} + \cos(\varphi_{\rm d}) \cdot y_{\rm c}. \tag{2}$$

In our case, since  $x_c = 0$  and  $y_c = R_s$ , (1 - 2) simplify to

$$x_{\rm nc} = -\sin(\varphi_{\rm d}) \cdot R_{\rm s},\tag{3}$$

$$y_{\rm nc} = \cos(\varphi_{\rm d}) \cdot R_{\rm s}. \tag{4}$$

The new, rotated cam circle equation is now

$$R_{\rm s}^2 = (x - x_{\rm nc})^2 + (y - y_{\rm nc})^2.$$
 (5)

To find the point  $(x_d, y_d)$ , we search for the intersection between the rotated cam circle from (5) and a line

$$y = \tan(-\pi/2 + \varphi_s) \cdot x + R_s. \tag{6}$$

going through point  $(x_c, y_c)$  with a slope of  $-\pi/2 + \varphi_s$ . The intersection point lies on  $(x_d, y_d)$ .

The point depends on the deflection angle  $\varphi_d$  and stiffness preset  $\varphi_s$ . With sin() and cos() shortened to s() and c(), we can express  $x_d$  and  $y_d$  as

$$x_{d} = \frac{R_{s}}{2} \left[ s(\varphi_{d} - 2\varphi_{s}) - s(\varphi_{d}) + s(2\varphi_{s}) \right] + \cdots$$

$$\cdots R_{s}s(\varphi_{s}) \sqrt{\frac{c(2\varphi_{s})}{2} + \frac{c(2\varphi_{d} - 2\varphi_{s})}{2} + c(\varphi_{d}) - c(\varphi_{d} - 2\varphi_{s})}, (7)$$

$$y_{d} = \frac{R_{s}}{2} \left[ 1 + c(\varphi_{d}) + c(\varphi_{d} - 2\varphi_{s}) - c(2\varphi_{s}) \right] - \cdots$$

$$\cdots R_{s}c(\varphi_{s}) \sqrt{\frac{c(2\varphi_{s})}{2} + \frac{c(2\varphi_{d} - 2\varphi_{s})}{2} + c(\varphi_{d}) - c(\varphi_{d} - 2\varphi_{s})}. (8)$$

The distance between coordinates  $(x_c, y_c)$  and the coordinates  $(x_d, y_d)$  can be calculated as

$$d_{\rm cd} = \sqrt{(x_{\rm d} - x_{\rm c})^2 + (y_{\rm d} - y_{\rm c})^2}.$$
 (9)

The spring compression is thus calculated as

$$d_{\rm spr} = R_{\rm s} - d_{\rm cd}.\tag{10}$$

It can be used in combination with the spring constant  $(k_{spr})$ of the linear compression spring in the stiffness mechanism to calculate the spring force

$$F_{\rm spr} = k_{\rm spr} \cdot d_{\rm spr}. \tag{11}$$

Lets define an auxiliary angle  $\delta$  as the slope of the line l, which goes through  $(x_d, y_d)$  and is perpendicular to the line going through  $(x_d, y_d)$  and  $(x_{nc}, y_{nc})$ , and being tangent to the cam circle curve,

$$\delta = \operatorname{atan}\left(\frac{y_{\rm d} - y_{\rm nc}}{x_{\rm d} - x_{\rm nc}}\right) + \frac{\pi}{2}.\tag{12}$$

The resultant force  $(F_{sum})$  can be calculated from the spring force  $(F_{\rm spr})$  and the pressure angle  $\alpha$  using the cosine function as

$$F_{\text{sum}} = \frac{F_{\text{spr}}}{\cos(\alpha)}$$
 and (13)  
 $\alpha = \delta - \varphi_{\text{s}}.$  (14)

$$\alpha = \delta - \varphi_{\rm s}. \tag{14}$$

In order to calculate the deflection torque  $M_d$ , the lever length (r) of the resultant force  $F_{\text{sum}}$  needs to be calculated (see Fig. 5). The lever (r) can be calculated using the cosine function

$$r = d_{\rm d} \cdot \cos(\gamma),$$
 (15)

$$d_{d} = \sqrt{x_{d}^{2} + y_{d}^{2}}, \qquad (16)$$

$$\gamma = \delta - \beta. \qquad (17)$$

$$\gamma = \delta - \beta. \tag{17}$$

Finally, the spring torque  $(M_s)$  in the simplest form is

$$M_{\rm s}(\varphi_{\rm s}, \varphi_{\rm d}) = F_{\rm sum} \cdot r, \tag{18}$$

where  $F_{\text{sum}}$  is from (13) and r the lever length from (15).

# C. Pseudo-linear behavior

Our use-case example, which also corresponds to the built physical prototype, was designed with specifications given in Table I.

TABLE I CALCULATION AND TEST PROTOTYPE PARAMETERS

Variable	Name	Value	Unit
$R_{\rm s}$	Cam curve radius	60	[mm]
$k_{\rm spr}$	Linear spring stiffness	9.5	[N/mm]
$arphi_{ m d}$	Deflection angle (min/max)	± 20	[°]
$\varphi_{\mathrm{s}}$	Stiffness setup angle range	0 - 45	[°]
$k_{\rm lin}$	Prototype max stiffness	0 - 16.3	[Nm/rad]
$M_{ m d}$	Prototype max def. torque	5.8	[Nm]
/	Prototype stiff. setup time	0.6 - 1.2	[s]

Fig. 6 shows the relation between the spring torque  $M_{\rm spr}$ (note that  $M_{\rm spr}=-M_{\rm d}$ ) and the passive deflection angle  $(\varphi_d)$ , calculated using the model (18), is nearly linear. The solid lines show the calculated results, while the dashed lines show a linear approximation for the different stiffness presets  $(\varphi_s)$ . A curve describing the relation between the stiffness  $k_{\rm lin}$  and the stiffness angle  $\varphi_s$  can be approximated from different presets of  $\varphi_s$ . The curve and the approximation are shown in Fig. 7 with a solid line and a dashed line, respectively. A 3rd order polynomial function was used in the approximation because it reduces the approximation error

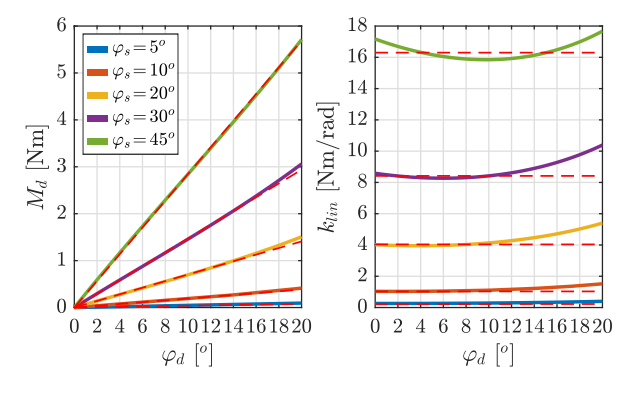


Fig. 6. Calculated torque-deflection characteristics for different stiffness preset angles  $(\varphi_s)$  with their linear approximations (dashed lines) left and right comparison between theoretical stiffness (colored) and linearly approximated stiffness (dashed). Pseudo-linear behavior can be observed.

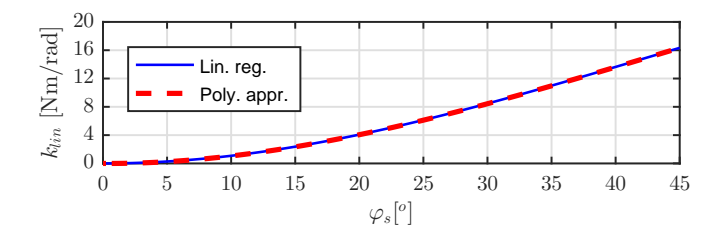


Fig. 7. Curve of approximated linear stiffness (klin) depending on the stiffness preset angle  $(\varphi_s)$ .

below the empirically chosen threshold of RMSE = 0.01(RMSE = 0.0056). For the given use case defined in Table I, it is

$$k_{lin}(\varphi_s) = -18.13\varphi_s^3 + 41.54\varphi_s^2 - 0.6598\varphi_s.$$
 (19)

Torque/deflection and stiffness/deflection plots in Fig. 6 show the pseudo-linear behavior of the proposed mechanism.

# D. Stiffness setup torque

Because of the pressure angle, described by (14), a tangential force ( $F_v$  in Fig. 3) has to be overcome to change the stiffness preset angle  $(\varphi_s)$ . This is the minimum boundary condition for the stiffness setup motor (see Fig. 1) torque. The amount of  $F_v$  on the roller stiffness mechanism can be calculated as

$$F_{\rm v} = F_{\rm spr} \cdot \tan \alpha. \tag{20}$$

Using the distance to the contact point on the deflection curve  $(d_{cd} \text{ in } (9))$  and the calculated  $F_{y}$ , the torque required to move the stiffness preset mechanism  $M_{\rm v}$  can be calculated as

$$M_{\rm v}(\varphi_{\rm s}, \varphi_{\rm d}) = d_{\rm cd} \cdot F_{\rm v}. \tag{21}$$

Note that  $M_{\rm v}$  depends on  $\varphi_{\rm s}$  and  $\varphi_{\rm d}$ .

# E. Comparing stiffness setup torque and deflection torque

A surface plot of external deflection torque  $(M_d)$  dependent on the deflection angle  $\varphi_{\rm d}$  and the stiffness preset angle  $\varphi_{\rm s}$ for our use case prototype with parameters given in Table I is shown on the left side of Fig. 8. On the right side of Fig. 8 we can see a surface plot for  $M_{\rm v}(\varphi_{\rm s}, \varphi_{\rm d})$ . The comparison of

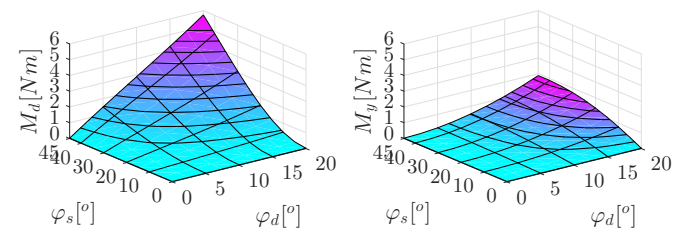


Fig. 8. Deflection torque  $M_{\rm d}(\varphi_{\rm s}, \varphi_{\rm d})$  as a function of the stiffness preset angle  $(\phi_s)$  and the deflection angle  $(\phi_d)$  on the left and the stiffness motor torque  $M_{\rm y}(\varphi_{\rm s},\varphi_{\rm d})$  on the right.

the surface plots in Fig. 8 shows that the deflection torque  $(M_{\rm d})$  is larger than the stiffness preset torque  $(M_{\rm v})$ , thus a weaker motor for stiffness setup can be used compared to the power of the position setup motor.

# F. Mechanisms principle main disadvantages

Looking at the working principle, one of the disadvantages is the slight discontinuity (non-linearity) when crossing the zero-deflection line. The discontinuity results from no load in the spring at the zero deflection. Consequently, there is no force to push on the cam roller, and it can slightly lift off. In order to minimize or prevent this, a tuning mechanism was implemented into the actuator to enable small, manual movement of the spring in order to fine-tune and minimize the zero crossing discontinuity.

Another problem is the stiffness preset torque, which is not constant. Due to the rising pressure angle, it increases with increased deflection, as seen in Fig. 9. It is the main parameter that limits the usable region in the deflection torque space and torque space of the stiffness motor (both seen in Fig. 8). The preferred working area depends upon the capabilities of the position and stiffness motors and needs to be considered during the control design. Similar can be observed in the AWAS-I actuator [18].

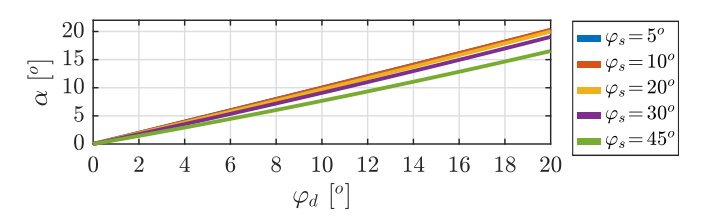


Fig. 9. Pressure angle for different stiffness presets.

The last issue stems from the fact that the elastic mechanism works in only one direction, meaning that a submechanism needs to be implemented, which is capable of changing the positive and negative deflection direction into merely one movement direction. In our rapid prototype, this was implemented using four gears and two deflection arms making the mechanism bidirectional. Other ways to achieve that are also possible, for example, with a pulley and cable transmission. In such case, only one lever arm is needed.

# IV. MEASUREMENTS

# A. Actuator prototype

In order to test our principle, a prototype actuator was developed using rapid prototyping. Plastics was chosen as the primary building material, keeping in mind that its properties are limited compared to metallic materials but sufficient for a test of concept. The use-case prototype is shown in Fig. 10. Two RC servos were used as drives. We used the Multiplex Royal BB servo motor (M = 0.8)Nm,  $\omega = 267$  deg/s at 4.8V) as the stiffness motor. A supplemental gear transmission (-3/1) increases its torque to 2.4 Nm and reduces its speed to 89 deg/s. Another servo (HITEC HS-755MG, M = 1.18 Nm,  $\omega$  = 214 deg/s) serves as position setup motor (see Fig. 1). With a supplemental gear (-31/25), its torque becomes 1.46 Nm and its speed reduces to 172 deg/s. Two additional incremental RLS RM22 rotation encoders were used to keep track of the stiffness setup angle  $(\varphi_s)$  and the deflection angle  $(\varphi_d)$  of the system.

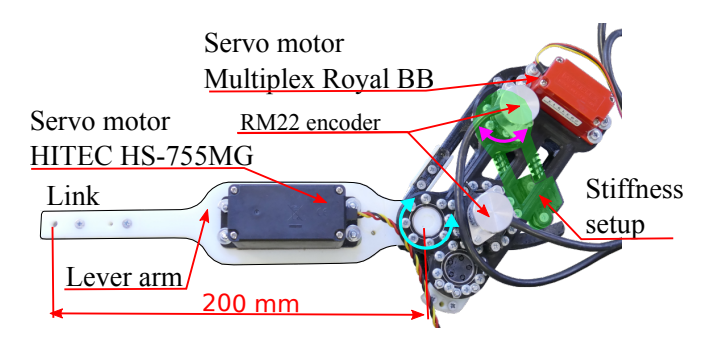


Fig. 10. Picture of the prototype PLVL-VSA actuator.

An Arduino MEGA board with a motor shield was used to drive the two servo motors. The servo motor position data was generated on a PC computer with Matlab-Simulink and then sent through serial communication onto the Arduino board. The encoder position was acquired using two encoder USB interfaces (RLS P201). The Simulink control loop was running with a frequency of 50 Hz, which was sufficient enough for the desired prototype evaluation.

#### B. Torque/deflection characteristics

In order to determine the torque/deflection characteristics of our actuator, a measurement system was designed consisting of a JR3 6-axis force/torque sensor mounted on a Mitsubishi PA-10 robot. An admittance force-feedback loop at 500 Hz was used to exert the desired forces onto the prototype PLVL-VSA actuator. The resulting measured forces were used to compare the theoretical deflection torque and the measured deflection torque (calculated from the measured forces). The comparison is shown in Figure 11.

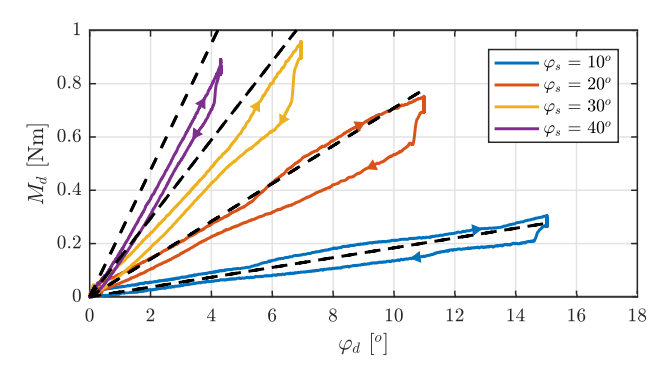


Fig. 11. Comparison between the theoretically approximated (dashed line) and actual deflection torque  $(M_{\rm d})$  for different stiffness presets. The arrows indicate the loading direction.

There is quite some discrepancy between the theoretical and the real data caused by nonlinearities like friction and backlash. This is to be expected since low-quality rapid prototyping parts were used. Most of prototype parts consist of plastics, so a lot of elastic material deformations are present. In addition, the RC servo motors are imprecise which also affects the setup of stiffness. Though, uncertainty persists in how much different nonlinearities contribute to the end result, the real signal behaves close to linear in the loading phase, which is a good enough result for the initial

prototype. Looking at the unloading phase, we can see that a torque hysteresis is present. The hysteresis is stronger in lower stiffness presets and smaller in higher presets. The exact cause of hysteresis is hard to determine. In higher stiffness presets and higher loads, the likely cause are the elastic deformations in the plastic material.

The main origin for hysteresis in the lower stiffness presets is expected to be the friction in bearings. Backlash is also present, due to the use of gears and imperfections in the plastic parts. However, all of these disadvantages can be either reduced or removed in the next actuator design iteration and with a more rigid, metallic design.

# C. Stiffness step response

Fast stiffness variation is desired in many applications, specifically in tasks that require contact with the environment and/or humans. A perpendicular stiffness variation mechanism is therefore most favorable since then the motor does not need to overcome the spring preload, meaning that all of the motors power can be used to vary the stiffness. In our case there is no resistance when varying the stiffness at zero deflection, except for the friction present in bearings and motor. Although, as the deflection angle increases, a resistive force results due to the pressure angle. As a consequence, stiffness variation speed is affected by the deflection angle  $(\varphi_d)$ . Our prototype used a hobby servo motor with limited output torque and rotation speed to change the stiffness.

Results of the step-change response of stiffness variation is shown in Fig. 12. The stiffness variation speed is between 0.6 s for small external load, shown with a small  $\varphi_d$ , and up to 1.2 s for a fully loaded mechanism. Using a stronger and faster motor, the stiffness variation time could be reduced.

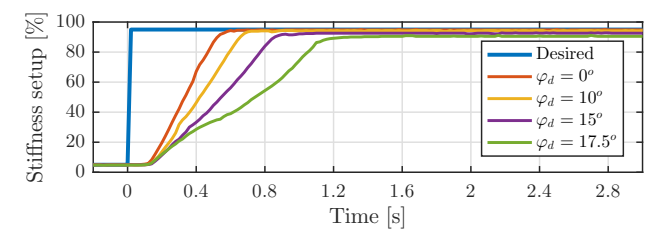


Fig. 12. Stiffness step response from 5% to 95% stiffness for different deflection angles  $(\phi_d).$ 

### V. CONCLUSIONS AND FUTURE WORK

The paper presents a novel design variation of a variable stiffness actuator, called the pseudo-linear variable-lever variable stiffness actuator, PLVL-VSA. The proposed actuator functions as a combination of a cam mechanism and a variable lever mechanism. Its main advantages are a rotational stiffness variation mechanism and pseudo-linear torque/deflection characteristics. The stiffness preset mechanism offers a reasonably fast stiffness change with a fairly weak motor since the stiffness change is utilized perpendicular to mechanism loading. Since stiffness is not varied through preload, the internal forces are kept lower, which enables a lighter, less rigid structure and allows the usage of a weaker stiffness-setup motor.

The stiffness setup and load are mechanically separated, allowing an individual setting of each. Accordingly, the control algorithms can be less complex. The torque/deflection characteristics is nearly linear, i.e., pseudo-linear, and can be approximated as linear, which simplifies the control design.

The design offers several courses of research for a future iteration of the actuator. One possibility is to replace the geared transmission with a cable transmission to reduce backlash and enable a more compact design. In the future, we will build a new prototype, using more powerful motors and more rigid structure materials. Furthermore, the next step will be to design a low-level controller. And lastly, the actuator will be used in an exoskeleton system to explore different higher-level control methods.

#### REFERENCES

- [1] G. Grioli, S. Wolf, *et al.*, "Variable stiffness actuators: The users point of view," *The International Journal of Robotics Research*, vol. 34, no. 6, pp. 727–743, 2015.
- [2] A. Albu-Schäffer, O. Eiberger, et al., "Soft robotics," *IEEE Robotics & Automation Mag.*, vol. 15, no. 3, pp. 20–30, 2008.
  [3] S. Wolf, G. Grioli, O. Eiberger, et al., "Variable stiffness actuators:
- [3] S. Wolf, G. Grioli, O. Eiberger, et al., "Variable stiffness actuators: Review on design and components," *IEEE/ASME Transactions on Mechatronics*, vol. 21, pp. 2418–2430, Oct 2016.
- [4] B. Vanderborght, A. Albu-Schäffer, et al., "Variable impedance actuators: A review," Robotics and autonomous systems, vol. 61, no. 12, pp. 1601–1614, 2013.
- [5] N. L. Tagliamonte, F. Sergi, et al., "Double actuation architectures for rendering variable impedance in compliant robots: A review," *Mechatronics*, vol. 22, no. 8, pp. 1187–1203, 2012.
- [6] R. Van Ham, T. Sugar, et al., "Review of actuators with passive adjustable compliance/controllable stiffness for robotic apllications," IEEE Robotics and Automation mag., vol. 16, no. 3, pp. 81–94, 2009.
- [7] R. Van Ham, B. Vanderborght, et al., "MACCEPA, the mechanically adjustable compliance and controllable equilibrium position actuator: Design and implementation in a biped robot," Robotics and Autonomous Systems, vol. 55, no. 10, pp. 761–768, 2007.
- [8] S. Wolf, O. Eiberger, and G. Hirzinger, "The DLR FSJ: Energy based design of a variable stiffness joint," in *IEEE International Conference* on Robotics and Automation (ICRA), pp. 5082–5089, IEEE, 2011.
- [9] T. Wimbock, C. Ott, A. Albu-Schaffer, A. Kugi, and G. Hirzinger, "Impedance control for variable stiffness mechanisms with nonlinear joint coupling," in *IEEE/RSJ International Conference on Intelligent Robots and Systems*, pp. 3796–3803, IEEE, 2008.
- [10] S. Wolf and G. Hirzinger, "A new variable stiffness design: Matching requirements of the next robot generation," in *International Conf. on Robotics and Automation (ICRA)*, pp. 1741–1746, IEEE, 2008.
- [11] K. L. Richards, Design Engineer's Handbook. CRC Press, 2012.
- [12] A. Jafari, N. G. Tsagarakis, et al., "AwAS-II: A new actuator with adjustable stiffness based on the novel principle of adaptable pivot point and variable lever ratio," in *IEEE International Conference on Robotics and Automation (ICRA)*, pp. 4638–4643, IEEE, 2011.
- [13] H. V. Quy, L. Aryananda, et al., "A novel mechanism for varying stiffness via changing transmission angle," in *International Conf. on Robotics and Automation (ICRA)*, pp. 5076–5081, IEEE, 2011.
- [14] B. Vanderborght, N. G. Tsagarakis, et al., "MACCEPA 2.0: compliant actuator used for energy efficient hopping robot Chobino1D," Autonomous Robots, vol. 31, no. 1, pp. 55–65, 2011.
- [15] M. Grebenstein, A. Albu-Schäffer, et al., "The DLR hand arm system," in *IEEE International Conference on Robotics and Automation (ICRA)*, pp. 3175–3182, IEEE, 2011.
- [16] P. Cherelle, V. Grosu, et al., "The MACCEPA actuation system as torque actuator in the gait rehabilitation robot ALTACRO," in 3rd IEEE RAS and EMBS International Conference on Biomedical Robotics and Biomechatronics (BioRob), pp. 27–32, IEEE, 2010.
- [17] VIACTORS homepage, "VSA data sheet." http://www.viactors.org/VSA%20data%20sheets.htm, 2012. [Online; accessed 9-February-2017].
- [18] A. Jafari, N. G. Tsagarakis, et al., "A novel actuator with adjustable stiffness (AwAS)," in IEEE/RSJ International Conference on Intelligent Robots and Systems (IROS), pp. 4201–4206, IEEE, 2010.